Supplementary Information

for

Time-Resolved X-Ray Scattering by Electronic Wave Packets:
Analytic Solutions to the Hydrogen Atom

Mats Simmermacher, Niels E. Henriksen, and Klaus B. Møller

Department of Chemistry, Technical University of Denmark,
2800 Kongens Lyngby, Denmark

(Dated: May 18, 2017)

Contents

S1 Inconsistent Waller-Hartree Approximation

In the following, the effect of an inconsistent application of the Waller-Hartree approximation $\omega_\mathrm{s} \approx \omega_0$ is discussed. As in the paper, the two scattering matrix elements in equation (2) become independent of ω_s. But instead of restricting the lower and upper limits of the remaining integral over ω_s to values in the vicinity of ω_0, the integral is assumed to run from zero to infinity, meaning that all scattered photons are detected regardless of their energies. Since the power spectral density $F\big(\omega_\mathrm{s} + \omega_{fij}\big)$ is normalized, the integral yields unity for every value of ω_{fij}. Hence, equation (2) becomes:

$$\frac{dS}{d\Omega} = \frac{d\sigma_\mathrm{t}}{d\Omega} \cdot \int_{-\infty}^{+\infty} I(t) \sum_{i,j} \sum_{f}^{\infty} c_i\, c_j^*\, e^{-\iota\omega_{ij}t}\, \tilde{L}_{fi}\, \tilde{L}_{fj}^*\, dt. \tag{S1}$$

In equation (S1), the scattering matrix elements summed over f are:

$$\sum_{f}^{\infty} \tilde{L}_{fi}\, \tilde{L}_{fj}^* = \sum_{f}^{\infty} \big\langle \boldsymbol{\psi}_j \big| \hat{\boldsymbol{L}}_0^\dagger \big| \boldsymbol{\psi}_f \big\rangle \big\langle \boldsymbol{\psi}_f \big| \hat{\boldsymbol{L}}_0 \big| \boldsymbol{\psi}_i \big\rangle. \tag{S2}$$

The zero in the subscript of $\hat{\boldsymbol{L}}_0$ labels the scattering operator to be independent of ω_s. By use of the resolution of the identity, $\boldsymbol{I} = \sum_f^\infty \big|\boldsymbol{\psi}_f\big\rangle\big\langle\boldsymbol{\psi}_f\big|$, equation (S2) simplifies to:

$$\sum_{f}^{\infty} \tilde{L}_{fi}\, \tilde{L}_{fj}^* = \big\langle \boldsymbol{\psi}_j \big| \hat{\boldsymbol{L}}_0^\dagger \hat{\boldsymbol{L}}_0 \big| \boldsymbol{\psi}_i \big\rangle = \sum_{m}^{N_\mathrm{e}} \sum_{n}^{N_\mathrm{e}} \big\langle \boldsymbol{\psi}_j \big| e^{\iota \boldsymbol{q}\cdot(\boldsymbol{r}_m - \boldsymbol{r}_n)} \big| \boldsymbol{\psi}_i \big\rangle. \tag{S3}$$

The two sums on the right-hand side of equation (S3) run over all N_e electrons. If both sums refer to the same electron, *i.e.* $m = n$, the exponential becomes unity. Thus, equation (S3) can be written as:

$$\begin{aligned} \sum_{f}^{\infty} \tilde{L}_{fi}\, \tilde{L}_{fj}^* &= N_\mathrm{e}\, \big\langle \boldsymbol{\psi}_j \big| \boldsymbol{\psi}_i \big\rangle + \sum_{m}^{N_\mathrm{e}} \sum_{n \neq m}^{N_\mathrm{e}} \big\langle \boldsymbol{\psi}_j \big| e^{\iota \boldsymbol{q}\cdot(\boldsymbol{r}_m - \boldsymbol{r}_n)} \big| \boldsymbol{\psi}_i \big\rangle \\ &= N_\mathrm{e}\, \delta_{ij} + \sum_{m}^{N_\mathrm{e}} \sum_{n \neq m}^{N_\mathrm{e}} \big\langle \boldsymbol{\psi}_j \big| e^{\iota \boldsymbol{q}\cdot(\boldsymbol{r}_m - \boldsymbol{r}_n)} \big| \boldsymbol{\psi}_i \big\rangle. \end{aligned} \tag{S4}$$

The Kronecker delta δ_{ij} in the second line of (S4) is a consequence of the orthonormality of the eigenstates $\big|\boldsymbol{\psi}_i\big\rangle$ and $\big|\boldsymbol{\psi}_j\big\rangle$. Equation (S1) can now be separated into a part that refers to single electrons, $dS_1/d\Omega$, and a part that involves pairs of different electrons, $dS_2/d\Omega$:

$$\frac{dS}{d\Omega} = \frac{dS_1}{d\Omega} + \frac{dS_2}{d\Omega}. \tag{S5}$$

With equation (S4), the two terms in (S5) are:

$$\frac{dS_1}{d\Omega} = \frac{d\sigma_\mathrm{t}}{d\Omega} \cdot \int_{-\infty}^{+\infty} I(t) \sum_{i,j} c_i\ c_j^*\ e^{-\iota\omega_{ij}t}\ N_\mathrm{e}\ \delta_{ij}\ dt = \frac{d\sigma_\mathrm{t}}{d\Omega}\ N_\mathrm{e}\ I, \tag{S6}$$

$$\begin{aligned}\frac{dS_2}{d\Omega} = \frac{d\sigma_\mathrm{t}}{d\Omega} \cdot \int_{-\infty}^{+\infty} I(t) \sum_{i,j} c_i\ c_j^*\ e^{-\iota\omega_{ij}t} \\ \times \sum_{m}^{N_\mathrm{e}} \sum_{n\neq m}^{N_\mathrm{e}} \left\langle \boldsymbol{\psi}_j \middle| e^{\iota \boldsymbol{q}\cdot(\boldsymbol{r}_m - \boldsymbol{r}_n)} \middle| \boldsymbol{\psi}_i \right\rangle\ dt.\end{aligned} \tag{S7}$$

Equation (S6) contains the total integrated intensity of the X-ray probe pulse, $I = \int_{-\infty}^{+\infty} I(t)\ dt$, and reveals that the scattering signal from single electrons is independent of both the time t and the $\boldsymbol{q}$-vector. It corresponds to the elastic scattering of N_e free electrons in a pulse with intensity I. Hence, the information contained in scattering by single bound electrons is lost. This is a direct consequence of the assumption that all scattered photons are detected without any energy resolution, which violates, strictly speaking, the condition under which the approximation $\omega_\mathrm{s} \approx \omega_0$ is justified.

S2 Derivation of Equations (17) and (18)

Here, equations (17) and (18) are derived. To begin with, the integrals of the scattering matrix element defined in equation (3) are written out explicitly:

$$L_{fi} = \int_{-\infty}^{\infty} \sum_{n=1}^{N_\mathrm{e}} e^{\iota \boldsymbol{q}\boldsymbol{r}_n} \cdot \boldsymbol{\psi}_f^*(\boldsymbol{r}_1 \ldots \boldsymbol{r}_N) \cdot \boldsymbol{\psi}_i(\boldsymbol{r}_1 \ldots \boldsymbol{r}_N)\; d\boldsymbol{r}_1 \ldots d\boldsymbol{r}_N. \quad \text{(S8)}$$

The sum and integrals in equation (S8) refer to all N_e electrons of the material system. Now, the exponential $e^{\iota \boldsymbol{q}\boldsymbol{r}_n}$ is expressed as an integral over a general electronic coordinate $\boldsymbol{r}$ by use of the sifting property of the Dirac delta function:

$$e^{\iota \boldsymbol{q}\boldsymbol{r}_n} = \int_{-\infty}^{\infty} e^{\iota \boldsymbol{q}\boldsymbol{r}} \cdot \delta(\boldsymbol{r} - \boldsymbol{r}_n)\; d\boldsymbol{r} \quad \text{(S9)}$$

An insertion of equation (S9) into equation (S8) yields after interchange of the order of the integrals:

$$L_{fi} = \int_{-\infty}^{\infty} e^{\iota \boldsymbol{q}\boldsymbol{r}} \cdot \sum_{n=1}^{N_\mathrm{e}} \left\langle \boldsymbol{\psi}_f \middle| \hat{\delta}(\boldsymbol{r} - \boldsymbol{r}_n) \middle| \boldsymbol{\psi}_i \right\rangle d\boldsymbol{r}. \quad \text{(S10)}$$

The Dirac delta function $\delta(\boldsymbol{r} - \boldsymbol{r}_n)$ in the matrix element on the right-hand side of equation (S10) sifts out the coordinates of one of the electrons:

$$\left\langle \boldsymbol{\psi}_f \middle| \hat{\delta}(\boldsymbol{r} - \boldsymbol{r}_n) \middle| \boldsymbol{\psi}_i \right\rangle = \int_{-\infty}^{\infty} \boldsymbol{\psi}_f^*(\boldsymbol{r}_1 \ldots \boldsymbol{r}_N) \cdot \boldsymbol{\psi}_i(\boldsymbol{r}_1 \ldots \boldsymbol{r}_N) \times d\boldsymbol{r}_1 \ldots d\boldsymbol{r}_{N-1}. \quad \text{(S11)}$$

Note that electrons are indistinguishable and hence the labeling of their coordinates $\boldsymbol{r}_n$ is arbitrary. The expression in equation (S10) involves the expectation value of the one-electron density operator $\rho_{fi}(\boldsymbol{r})$ given in equation (15) in its Fourier transform $\mathcal{F}_{\boldsymbol{r}}\left[\rho_{fi}(\boldsymbol{r})\right](\boldsymbol{q})$ from $\boldsymbol{r}$- into $\boldsymbol{q}$-space defined in equation (16). Hence, equation (S10) can be written as:

$$L_{fi} = \mathcal{F}_{\boldsymbol{r}}\left[\rho_{fi}(\boldsymbol{r})\right](\boldsymbol{q}). \quad \text{(S12)}$$

By insertion of equation (S12) into the scattering matrix elements in equations (7) and (10), equations (17) and (18) are obtained.

S3 Expansion of Atomic Orbitals

Tab. S1: Atomic orbitals with principal quantum numbers $n \in \{1,2,3,4\}$ expressed as linear combinations of complex parabolic eigenstates $\boldsymbol{\psi}_{n,n_1,n_2}(\xi,\eta,\varphi)$. The latter are written as $\lvert \boldsymbol{n, n_1, n_2}\rangle$, where n_1 and n_2 are parabolic quantum numbers that obey the relation $n = n_1 + n_2 + m + 1$. m is the magnetic quantum number.

orbitals	**linear combination of parabolic eigenstates**
$\lvert\mathbf{1s}\rangle$	$\lvert\mathbf{1,0,0}\rangle$
$\lvert\mathbf{2s}\rangle$	$\frac{1}{\sqrt{2}} \cdot \left[\lvert\mathbf{2,1,0}\rangle + \lvert\mathbf{2,0,1}\rangle\right]$
$\lvert\mathbf{2p}_x\rangle$	$\frac{1}{\sqrt{2}} \cdot \left[\lvert\mathbf{2,0,0}\rangle^* + \lvert\mathbf{2,0,0}\rangle\right]$
$\lvert\mathbf{2p}_y\rangle$	$\frac{\imath}{\sqrt{2}} \cdot \left[\lvert\mathbf{2,0,0}\rangle^* - \lvert\mathbf{2,0,0}\rangle\right]$
$\lvert\mathbf{2p}_z\rangle$	$\frac{1}{\sqrt{2}} \cdot \left[\lvert\mathbf{2,1,0}\rangle - \lvert\mathbf{2,0,1}\rangle\right]$
$\lvert\mathbf{3s}\rangle$	$\frac{1}{\sqrt{3}} \cdot \left[\lvert\mathbf{3,2,0}\rangle + \lvert\mathbf{3,1,1}\rangle + \lvert\mathbf{3,0,2}\rangle\right]$
$\lvert\mathbf{3p}_x\rangle$	$\frac{1}{\sqrt{4}} \cdot \left[\lvert\mathbf{3,1,0}\rangle^* + \lvert\mathbf{3,1,0}\rangle + \lvert\mathbf{3,0,1}\rangle^* + \lvert\mathbf{3,0,1}\rangle\right]$
$\lvert\mathbf{3p}_y\rangle$	$\frac{\imath}{\sqrt{4}} \cdot \left[\lvert\mathbf{3,1,0}\rangle^* - \lvert\mathbf{3,1,0}\rangle + \lvert\mathbf{3,0,1}\rangle^* - \lvert\mathbf{3,0,1}\rangle\right]$
$\lvert\mathbf{3p}_z\rangle$	$\frac{1}{\sqrt{2}} \cdot \left[\lvert\mathbf{3,2,0}\rangle - \lvert\mathbf{3,0,2}\rangle\right]$
$\lvert\mathbf{3d}_{x^2-y^2}\rangle$	$\frac{1}{\sqrt{2}} \cdot \left[\lvert\mathbf{3,0,0}\rangle^* + \lvert\mathbf{3,0,0}\rangle\right]$
$\lvert\mathbf{3d}_{xy}\rangle$	$\frac{\imath}{\sqrt{2}} \cdot \left[\lvert\mathbf{3,0,0}\rangle^* - \lvert\mathbf{3,0,0}\rangle\right]$
$\lvert\mathbf{3d}_{xz}\rangle$	$\frac{1}{\sqrt{4}} \cdot \left[\lvert\mathbf{3,1,0}\rangle^* + \lvert\mathbf{3,1,0}\rangle - \lvert\mathbf{3,0,1}\rangle^* - \lvert\mathbf{3,0,1}\rangle\right]$
$\lvert\mathbf{3d}_{yz}\rangle$	$\frac{\imath}{\sqrt{4}} \cdot \left[\lvert\mathbf{3,1,0}\rangle^* - \lvert\mathbf{3,1,0}\rangle - \lvert\mathbf{3,0,1}\rangle^* + \lvert\mathbf{3,0,1}\rangle\right]$
$\lvert\mathbf{3d}_z^2\rangle$	$\frac{1}{\sqrt{6}} \cdot \left[\lvert\mathbf{3,2,0}\rangle - 2 \cdot \lvert\mathbf{3,1,1}\rangle + \lvert\mathbf{3,0,2}\rangle\right]$
$\lvert\mathbf{4s}\rangle$	$\frac{1}{\sqrt{4}} \cdot \left[\lvert\mathbf{4,3,0}\rangle + \lvert\mathbf{4,0,3}\rangle + \lvert\mathbf{4,2,1}\rangle + \lvert\mathbf{4,1,2}\rangle\right]$
$\lvert\mathbf{4p}_x\rangle$	$\frac{1}{\sqrt{5}} \cdot \left[\frac{\sqrt{3}}{2} \cdot \left(\lvert\mathbf{4,2,0}\rangle^* + \lvert\mathbf{4,2,0}\rangle + \lvert\mathbf{4,0,2}\rangle^* + \lvert\mathbf{4,0,2}\rangle\right) + \lvert\mathbf{4,1,1}\rangle^* + \lvert\mathbf{4,1,1}\rangle\right]$
$\lvert\mathbf{4p}_y\rangle$	$\frac{\imath}{\sqrt{5}} \cdot \left[\frac{\sqrt{3}}{2} \cdot \left(\lvert\mathbf{4,2,0}\rangle^* - \lvert\mathbf{4,2,0}\rangle + \lvert\mathbf{4,0,2}\rangle^* - \lvert\mathbf{4,0,2}\rangle\right) + \lvert\mathbf{4,1,1}\rangle^* - \lvert\mathbf{4,1,1}\rangle\right]$
$\lvert\mathbf{4p}_z\rangle$	$\frac{1}{2\sqrt{5}} \cdot \left[3 \cdot \left(\lvert\mathbf{4,3,0}\rangle - \lvert\mathbf{4,0,3}\rangle\right) + \lvert\mathbf{4,2,1}\rangle - \lvert\mathbf{4,1,2}\rangle\right]$
$\lvert\mathbf{4d}_{x^2-y^2}\rangle$	$\frac{1}{\sqrt{4}} \cdot \left[\lvert\mathbf{4,1,0}\rangle^* + \lvert\mathbf{4,1,0}\rangle + \lvert\mathbf{4,0,1}\rangle^* + \lvert\mathbf{4,0,1}\rangle\right]$
$\lvert\mathbf{4d}_{xy}\rangle$	$\frac{\imath}{\sqrt{4}} \cdot \left[\lvert\mathbf{4,1,0}\rangle^* - \lvert\mathbf{4,1,0}\rangle + \lvert\mathbf{4,0,1}\rangle^* - \lvert\mathbf{4,0,1}\rangle\right]$
$\lvert\mathbf{4d}_{xz}\rangle$	$\frac{1}{\sqrt{4}} \cdot \left[\lvert\mathbf{4,2,0}\rangle^* + \lvert\mathbf{4,2,0}\rangle - \lvert\mathbf{4,0,2}\rangle^* - \lvert\mathbf{4,0,2}\rangle\right]$
$\lvert\mathbf{4d}_{yz}\rangle$	$\frac{\imath}{\sqrt{4}} \cdot \left[\lvert\mathbf{4,2,0}\rangle^* - \lvert\mathbf{4,2,0}\rangle - \lvert\mathbf{4,0,2}\rangle^* + \lvert\mathbf{4,0,2}\rangle\right]$
$\lvert\mathbf{4d}_{z^2}\rangle$	$\frac{1}{\sqrt{4}} \cdot \left[\lvert\mathbf{4,3,0}\rangle + \lvert\mathbf{4,0,3}\rangle - \lvert\mathbf{4,2,1}\rangle - \lvert\mathbf{4,1,2}\rangle\right]$
$\lvert\mathbf{4f}_{x(x^2-3y^2)}\rangle$	$\frac{1}{\sqrt{2}} \cdot \left[\lvert\mathbf{4,0,0}\rangle^* + \lvert\mathbf{4,0,0}\rangle\right]$
$\lvert\mathbf{4f}_{y(3x^2-y^2)}\rangle$	$\frac{\imath}{\sqrt{2}} \cdot \left[\lvert\mathbf{4,0,0}\rangle^* - \lvert\mathbf{4,0,0}\rangle\right]$
$\lvert\mathbf{4f}_{z(x^2-y^2)}\rangle$	$\frac{1}{\sqrt{4}} \cdot \left[\lvert\mathbf{4,1,0}\rangle^* + \lvert\mathbf{4,1,0}\rangle - \lvert\mathbf{4,0,1}\rangle^* - \lvert\mathbf{4,0,1}\rangle\right]$
$\lvert\mathbf{4f}_{xyz}\rangle$	$\frac{\imath}{\sqrt{4}} \cdot \left[\lvert\mathbf{4,1,0}\rangle^* - \lvert\mathbf{4,1,0}\rangle - \lvert\mathbf{4,0,1}\rangle^* + \lvert\mathbf{4,0,1}\rangle\right]$
$\lvert\mathbf{4f}_{xz^2}\rangle$	$\frac{1}{\sqrt{10}} \cdot \left[\lvert\mathbf{4,2,0}\rangle^* + \lvert\mathbf{4,2,0}\rangle + \lvert\mathbf{4,0,2}\rangle^* + \lvert\mathbf{4,0,2}\rangle - \sqrt{3} \cdot \left(\lvert\mathbf{4,1,1}\rangle^* + \lvert\mathbf{4,1,1}\rangle\right)\right]$
$\lvert\mathbf{4f}_{yz^2}\rangle$	$\frac{\imath}{\sqrt{10}} \cdot \left[\lvert\mathbf{4,2,0}\rangle^* - \lvert\mathbf{4,2,0}\rangle + \lvert\mathbf{4,0,2}\rangle^* - \lvert\mathbf{4,0,2}\rangle - \sqrt{3} \cdot \left(\lvert\mathbf{4,1,1}\rangle^* - \lvert\mathbf{4,1,1}\rangle\right)\right]$
$\lvert\mathbf{4f}_{z^3}\rangle$	$\frac{1}{2\sqrt{5}} \cdot \left[\lvert\mathbf{4,3,0}\rangle - \lvert\mathbf{4,0,3}\rangle - 3 \cdot \left(\lvert\mathbf{4,2,1}\rangle - \lvert\mathbf{4,1,2}\rangle\right)\right]$

S4 Rotation of Atomic Orbitals

Here, the rotation of an atomic $\left|\boldsymbol{n}\mathbf{d}_{z^2}\right\rangle$ orbital is demonstrated in detail. First, the rotation matrix $\hat{\mathbf{R}}_y(\theta)$ acts upon the orbital and thereby transforms the z-coordinate as $z \rightarrow \sin(\theta) \cdot x + \cos(\theta) \cdot z$:

$$\begin{aligned}\hat{\mathbf{R}}_y(\theta)\ \left|\boldsymbol{n}\mathbf{d}_{z^2}\right\rangle &= \left[\sin(\theta) \cdot \left|\boldsymbol{n}\tilde{\mathbf{d}}_x\right\rangle + \cos(\theta) \cdot \left|\boldsymbol{n}\tilde{\mathbf{d}}_z\right\rangle\right]^2 \\ &= \left[\sin^2(\theta) \cdot \left|\boldsymbol{n}\tilde{\mathbf{d}}_{x^2}\right\rangle + \sin(2\theta) \cdot \left|\boldsymbol{n}\tilde{\mathbf{d}}_{xz}\right\rangle \right. \\ &\quad \left. + \cos^2(\theta) \cdot \left|\boldsymbol{n}\tilde{\mathbf{d}}_{z^2}\right\rangle\right].\end{aligned} \tag{S13}$$

The vector $\left|\boldsymbol{n}\tilde{\mathbf{d}}_{x^2}\right\rangle$ can be expressed as a proper linear combination of the common set of atomic $\left|\mathbf{d}\right\rangle$ orbitals, as shown in table S2. The tilde on top of $\tilde{\mathbf{d}}$ denotes that the vector has to be multiplied with an additional factor so that $\left|\boldsymbol{n}\mathbf{d}_{z^2}\right\rangle$ remains normalized under rotation. The same holds for all other states following this notation. Now, the operator $\hat{\mathbf{R}}_z(\phi)$ acts upon the vectors in the second and third line of equation (S13):

$$\begin{aligned}\hat{\mathbf{R}}_z(\phi)\ \left|\boldsymbol{n}\tilde{\mathbf{d}}_{x^2}\right\rangle &= \left[\cos^2(\phi) \cdot \left|\boldsymbol{n}\tilde{\mathbf{d}}_{x^2}\right\rangle + \sin(2\phi) \cdot \left|\boldsymbol{n}\tilde{\mathbf{d}}_{xy}\right\rangle \right. \\ &\quad \left. + \sin^2(\phi) \cdot \left|\boldsymbol{n}\tilde{\mathbf{d}}_{y^2}\right\rangle\right],\end{aligned} \tag{S14}$$

$$\hat{\mathbf{R}}_z(\phi)\ \left|\boldsymbol{n}\tilde{\mathbf{d}}_{xz}\right\rangle = \left[\cos(\phi) \cdot \left|\boldsymbol{n}\tilde{\mathbf{d}}_{xz}\right\rangle + \sin(\phi) \cdot \left|\boldsymbol{n}\tilde{\mathbf{d}}_{yz}\right\rangle\right], \tag{S15}$$

$$\hat{\mathbf{R}}_z(\phi)\ \left|\boldsymbol{n}\tilde{\mathbf{d}}_{z^2}\right\rangle = \left|\boldsymbol{n}\tilde{\mathbf{d}}_{z^2}\right\rangle. \tag{S16}$$

The function $\left|\boldsymbol{n}\mathbf{d}_{z^2;\mathbf{R}}(\theta,\phi)\right\rangle$ that represents the rotation of the $\left|\boldsymbol{n}\mathbf{d}_{z^2}\right\rangle$ orbital is obtainable by combination of equation (S13) with equations (S14) to (S16):

$$\begin{aligned}\left|\boldsymbol{n}\mathbf{d}_{z^2;\mathbf{R}}(\theta,\phi)\right\rangle = \sin^2(\theta) &\cdot \left[\cos^2(\phi) \cdot \left|\boldsymbol{n}\tilde{\mathbf{d}}_{x^2}\right\rangle + \sin(2\phi) \cdot \left|\boldsymbol{n}\tilde{\mathbf{d}}_{xy}\right\rangle \right. \\ &\quad \left. + \sin^2(\phi) \cdot \left|\boldsymbol{n}\tilde{\mathbf{d}}_{y^2}\right\rangle\right] \\ &+ \sin(2\theta) \cdot \left[\cos(\phi) \cdot \left|\boldsymbol{n}\tilde{\mathbf{d}}_{xz}\right\rangle + \sin(\phi) \cdot \left|\boldsymbol{n}\tilde{\mathbf{d}}_{yz}\right\rangle\right] \\ &+ \cos^2(\theta) \cdot \left|\boldsymbol{n}\tilde{\mathbf{d}}_{z^2}\right\rangle.\end{aligned} \tag{S17}$$

Finally, the vectors on the right-hand side of equation (S17) can be substituted by their corresponding linear combinations of atomic orbitals given in table S2. After a rearrangement of terms, the equation for $\left|\boldsymbol{n}\mathbf{d}_{z^2;\mathbf{R}}(\theta,\phi)\right\rangle$ in table S3 is obtained. All other rotations of atomic orbitals provided in tables S3 to S4.2 have been derived in the same way.

Tab. S2: Vectors $\left|\boldsymbol{n}\tilde{\boldsymbol{l}}_\pi\right\rangle$ with $\pi = \prod_i^l \alpha_i$ and $\alpha_i \in \{x, y, z\}$ expressed as linear combinations of real-valued atomic orbitals for arbitrary principal quantum numbers n and azimuthal quantum numbers of $l = 2$ (**d**) and $l = 3$ (**f**). The factors have been chosen in order to conserve the normalization of $\left|\boldsymbol{n}\mathbf{d}_{z^2}\right\rangle$ and $\left|\boldsymbol{n}\mathbf{f}_{z^3}\right\rangle$ under rotation. If other atomic orbitals are rotated, these factors have to be modified accordingly.

component	linear combination of atomic orbitals
$\left\|\boldsymbol{n}\tilde{\mathbf{d}}_{x^2}\right\rangle$	$\frac{\sqrt{3}}{2} \cdot \left\|\boldsymbol{n}\mathbf{d}_{x^2-y^2}\right\rangle - \frac{1}{2} \cdot \left\|\boldsymbol{n}\mathbf{d}_{z^2}\right\rangle$
$\left\|\boldsymbol{n}\tilde{\mathbf{d}}_{y^2}\right\rangle$	$-\frac{\sqrt{3}}{2} \cdot \left\|\boldsymbol{n}\mathbf{d}_{x^2-y^2}\right\rangle - \frac{1}{2} \cdot \left\|\boldsymbol{n}\mathbf{d}_{z^2}\right\rangle$
$\left\|\boldsymbol{n}\tilde{\mathbf{d}}_{z^2}\right\rangle$	$\left\|\boldsymbol{n}\mathbf{d}_{z^2}\right\rangle$
$\left\|\boldsymbol{n}\tilde{\mathbf{d}}_{xy}\right\rangle$	$\frac{\sqrt{3}}{2} \cdot \left\|\boldsymbol{n}\mathbf{d}_{xy}\right\rangle$
$\left\|\boldsymbol{n}\tilde{\mathbf{d}}_{xz}\right\rangle$	$\frac{\sqrt{3}}{2} \cdot \left\|\boldsymbol{n}\mathbf{d}_{xz}\right\rangle$
$\left\|\boldsymbol{n}\tilde{\mathbf{d}}_{yz}\right\rangle$	$\frac{\sqrt{3}}{2} \cdot \left\|\boldsymbol{n}\mathbf{d}_{yz}\right\rangle$
$\left\|\boldsymbol{n}\tilde{\mathbf{f}}_{x^3}\right\rangle$	$\sqrt{\frac{5}{8}} \cdot \left\|\boldsymbol{n}\mathbf{f}_{x(x^2-3y^2)}\right\rangle - \sqrt{\frac{3}{8}} \cdot \left\|\boldsymbol{n}\mathbf{f}_{xz^2}\right\rangle$
$\left\|\boldsymbol{n}\tilde{\mathbf{f}}_{y^3}\right\rangle$	$-\sqrt{\frac{5}{8}} \cdot \left\|\boldsymbol{n}\mathbf{f}_{y(3x^2-y^2)}\right\rangle - \sqrt{\frac{3}{8}} \cdot \left\|\boldsymbol{n}\mathbf{f}_{yz^2}\right\rangle$
$\left\|\boldsymbol{n}\tilde{\mathbf{f}}_{z^3}\right\rangle$	$\left\|\boldsymbol{n}\mathbf{f}_{z^3}\right\rangle$
$\left\|\boldsymbol{n}\tilde{\mathbf{f}}_{x^2y}\right\rangle$	$\sqrt{\frac{5}{8}} \cdot \left\|\boldsymbol{n}\mathbf{f}_{y(3x^2-y^2)}\right\rangle - \frac{1}{\sqrt{24}} \cdot \left\|\boldsymbol{n}\mathbf{f}_{yz^2}\right\rangle$
$\left\|\boldsymbol{n}\tilde{\mathbf{f}}_{x^2z}\right\rangle$	$\sqrt{\frac{5}{12}} \cdot \left\|\boldsymbol{n}\mathbf{f}_{z(x^2-y^2)}\right\rangle - \frac{1}{2} \cdot \left\|\boldsymbol{n}\mathbf{f}_{z^3}\right\rangle$
$\left\|\boldsymbol{n}\tilde{\mathbf{f}}_{xy^2}\right\rangle$	$-\sqrt{\frac{5}{8}} \cdot \left\|\boldsymbol{n}\mathbf{f}_{x(x^2-3y^2)}\right\rangle - \frac{1}{\sqrt{24}} \cdot \left\|\boldsymbol{n}\mathbf{f}_{xz^2}\right\rangle$
$\left\|\boldsymbol{n}\tilde{\mathbf{f}}_{xz^2}\right\rangle$	$\sqrt{\frac{2}{3}} \cdot \left\|\boldsymbol{n}\mathbf{f}_{xz^2}\right\rangle$
$\left\|\boldsymbol{n}\tilde{\mathbf{f}}_{y^2z}\right\rangle$	$-\sqrt{\frac{5}{12}} \cdot \left\|\boldsymbol{n}\mathbf{f}_{z(x^2-y^2)}\right\rangle - \frac{1}{2} \cdot \left\|\boldsymbol{n}\mathbf{f}_{z^3}\right\rangle$
$\left\|\boldsymbol{n}\tilde{\mathbf{f}}_{yz^2}\right\rangle$	$\sqrt{\frac{2}{3}} \cdot \left\|\boldsymbol{n}\mathbf{f}_{yz^2}\right\rangle$
$\left\|\boldsymbol{n}\tilde{\mathbf{f}}_{xyz}\right\rangle$	$\sqrt{\frac{5}{12}} \cdot \left\|\boldsymbol{n}\mathbf{f}_{xyz}\right\rangle$

Tab. S3: Rotation of atomic $|\mathbf{d}\rangle$ orbitals with arbitrary principal quantum number n by polar and azimuthal angles of θ and ϕ, respectively. The rotations are expressed as angle-dependent linear combinations of atomic orbitals that share the same principal and azimuthal quantum numbers n and $l = 2$. The coefficients have been derived by operation of the rotation matrices $\hat{\mathbf{R}}_y(\theta)$ and $\hat{\mathbf{R}}_z(\phi)$ upon $|\mathbf{d}\rangle$.

	orbitals	**angle-dependent coefficients**
$\lvert n\mathbf{d}_{x^2-y^2;\mathbf{R}}(\theta,\phi)\rangle$	$\lvert n\mathbf{d}_{x^2-y^2}\rangle$	$\frac{1}{2}\cdot\left[\cos^2(\theta)+1\right]\cdot\cos(2\phi)$
	$\lvert n\mathbf{d}_{xy}\rangle$	$\left[\cos^2(\theta)+1\right]\cdot\sin(\phi)\,\cos(\phi)$
	$\lvert n\mathbf{d}_{xz}\rangle$	$-\sin(\theta)\,\cos(\theta)\,\cos(\phi)$
	$\lvert n\mathbf{d}_{yz}\rangle$	$-\sin(\theta)\,\cos(\theta)\,\sin(\phi)$
	$\lvert n\mathbf{d}_{z^2}\rangle$	$\frac{\sqrt{3}}{2}\,\sin^2(\theta)$
$\lvert n\mathbf{d}_{xy;\mathbf{R}}(\theta,\phi)\rangle$	$\lvert n\mathbf{d}_{x^2-y^2}\rangle$	$-2\,\cos(\theta)\,\sin(\phi)\,\cos(\phi)$
	$\lvert n\mathbf{d}_{xy}\rangle$	$\cos(\theta)\,\cos(2\phi)$
	$\lvert n\mathbf{d}_{xz}\rangle$	$\sin(\theta)\,\sin(\phi)$
	$\lvert n\mathbf{d}_{yz}\rangle$	$-\sin(\theta)\,\cos(\phi)$
	$\lvert n\mathbf{d}_{z^2}\rangle$	0
$\lvert n\mathbf{d}_{xz;\mathbf{R}}(\theta,\phi)\rangle$	$\lvert n\mathbf{d}_{x^2-y^2}\rangle$	$\cos(\theta)\,\sin(\theta)\,\cos(2\phi)$
	$\lvert n\mathbf{d}_{xy}\rangle$	$2\,\cos(\theta)\,\sin(\theta)\,\sin(\phi)\,\cos(\phi)$
	$\lvert n\mathbf{d}_{xz}\rangle$	$\cos(2\theta)\,\cos(\phi)$
	$\lvert n\mathbf{d}_{yz}\rangle$	$\cos(2\theta)\,\sin(\phi)$
	$\lvert n\mathbf{d}_{z^2}\rangle$	$-\sqrt{3}\,\sin(\theta)\,\cos(\theta)$
$\lvert n\mathbf{d}_{yz;\mathbf{R}}(\theta,\phi)\rangle$	$\lvert n\mathbf{d}_{x^2-y^2}\rangle$	$-2\,\sin(\theta)\,\sin(\phi)\,\cos(\phi)$
	$\lvert n\mathbf{d}_{xy}\rangle$	$\sin(\theta)\,\cos(2\phi)$
	$\lvert n\mathbf{d}_{xz}\rangle$	$-\cos(\theta)\,\sin(\phi)$
	$\lvert n\mathbf{d}_{yz}\rangle$	$\cos(\theta)\,\cos(\phi)$
	$\lvert n\mathbf{d}_{z^2}\rangle$	0
$\lvert n\mathbf{d}_{z^2;\mathbf{R}}(\theta,\phi)\rangle$	$\lvert n\mathbf{d}_{x^2-y^2}\rangle$	$\frac{\sqrt{3}}{2}\,\sin^2(\theta)\,\cos(2\phi)$
	$\lvert n\mathbf{d}_{xy}\rangle$	$\sqrt{3}\,\sin^2(\theta)\,\sin(\phi)\,\cos(\phi)$
	$\lvert n\mathbf{d}_{xz}\rangle$	$\sqrt{3}\,\sin(\theta)\,\cos(\theta)\,\cos(\phi)$
	$\lvert n\mathbf{d}_{yz}\rangle$	$\sqrt{3}\,\sin(\theta)\,\cos(\theta)\,\sin(\phi)$
	$\lvert n\mathbf{d}_{z^2}\rangle$	$\frac{1}{4}\cdot\left[3\,\cos(2\theta)+1\right]$

Tab. S4.1: Rotation of atomic $|\mathbf{f}\rangle$ orbitals with arbitrary principal quantum number n by polar and azimuthal angles of θ and ϕ, respectively. The rotations are expressed as angle-dependent linear combinations of atomic orbitals that share the same principal and azimuthal quantum numbers n and $l = 3$. The coefficients have been derived by operation of the rotation matrices $\hat{\mathbf{R}}_y(\theta)$ and $\hat{\mathbf{R}}_z(\phi)$ upon $|\mathbf{f}\rangle$.

	orbitals	**angle-dependent coefficients**
$\lvert \boldsymbol{n}\mathbf{f}_{x(x^2-3y^2);\mathbf{R}}(\theta,\phi)\rangle$	$\lvert \boldsymbol{n}\mathbf{f}_{x(x^2-3y^2)}\rangle$	$\frac{1}{16} \cdot \left[15\,\cos(\theta) + \cos(3\theta)\right] \cdot \cos(3\phi)$
	$\lvert \boldsymbol{n}\mathbf{f}_{y(3x^2-y^2)}\rangle$	$\frac{1}{16} \cdot \left[15\,\cos(\theta) + \cos(3\theta)\right] \cdot \sin(3\phi)$
	$\lvert \boldsymbol{n}\mathbf{f}_{z(x^2-y^2)}\rangle$	$-\sqrt{\frac{3}{8}}\,\sin(\theta) \cdot \left[\cos^2(\theta) + 1\right] \cdot \cos(2\phi)$
	$\lvert \boldsymbol{n}\mathbf{f}_{xyz}\rangle$	$-\sqrt{\frac{3}{2}}\,\sin(\theta) \cdot \left[\cos^2(\theta) + 1\right] \cdot \sin(\phi)\,\cos(\phi)$
	$\lvert \boldsymbol{n}\mathbf{f}_{xz^2}\rangle$	$\frac{\sqrt{15}}{4}\,\sin^2(\theta)\,\cos(\theta)\,\cos(\phi)$
	$\lvert \boldsymbol{n}\mathbf{f}_{yz^2}\rangle$	$\frac{\sqrt{15}}{4}\,\sin^2(\theta)\,\cos(\theta)\,\sin(\phi)$
	$\lvert \boldsymbol{n}\mathbf{f}_{z^3}\rangle$	$-\sqrt{\frac{5}{8}}\,\sin^3(\theta)$
$\lvert \boldsymbol{n}\mathbf{f}_{y(3x^2-y^2);\mathbf{R}}(\theta,\phi)\rangle$	$\lvert \boldsymbol{n}\mathbf{f}_{x(x^2-3y^2)}\rangle$	$-\frac{1}{4} \cdot \left[3\,\cos^2(\theta) + 1\right] \cdot \sin(3\phi)$
	$\lvert \boldsymbol{n}\mathbf{f}_{y(3x^2-y^2)}\rangle$	$\frac{1}{4} \cdot \left[3\,\cos^2(\theta) + 1\right] \cdot \cos(3\phi)$
	$\lvert \boldsymbol{n}\mathbf{f}_{z(x^2-y^2)}\rangle$	$\sqrt{6}\,\sin(\theta)\,\cos(\theta)\,\sin(\phi)\,\cos(\phi)$
	$\lvert \boldsymbol{n}\mathbf{f}_{xyz}\rangle$	$-\sqrt{\frac{3}{2}}\,\sin(\theta)\,\cos(\theta)\,\cos(2\phi)$
	$\lvert \boldsymbol{n}\mathbf{f}_{xz^2}\rangle$	$-\frac{\sqrt{15}}{4}\,\sin^2(\theta)\,\sin(\phi)$
	$\lvert \boldsymbol{n}\mathbf{f}_{yz^2}\rangle$	$\frac{\sqrt{15}}{4}\,\sin^2(\theta)\,\cos(\phi)$
	$\lvert \boldsymbol{n}\mathbf{f}_{z^3}\rangle$	0
$\lvert \boldsymbol{n}\mathbf{f}_{z(x^2-y^2);\mathbf{R}}(\theta,\phi)\rangle$	$\lvert \boldsymbol{n}\mathbf{f}_{x(x^2-3y^2)}\rangle$	$\sqrt{\frac{3}{8}}\,\sin(\theta) \cdot \left[\cos^2(\theta) + 1\right] \cdot \cos(3\phi)$
	$\lvert \boldsymbol{n}\mathbf{f}_{y(3x^2-y^2)}\rangle$	$\sqrt{\frac{3}{8}}\,\sin(\theta) \cdot \left[\cos^2(\theta) + 1\right] \cdot \sin(3\phi)$
	$\lvert \boldsymbol{n}\mathbf{f}_{z(x^2-y^2)}\rangle$	$-\frac{1}{2} \cdot \left[\cos(\theta) - 3\,\cos^3(\theta)\right] \cdot \cos(2\phi)$
	$\lvert \boldsymbol{n}\mathbf{f}_{xyz}\rangle$	$-\left[\cos(\theta) - 3\,\cos^3(\theta)\right] \cdot \sin(\phi)\,\cos(\phi)$
	$\lvert \boldsymbol{n}\mathbf{f}_{xz^2}\rangle$	$-\frac{1}{8}\sqrt{\frac{5}{2}} \cdot \left[3\,\sin(3\theta) - \sin(\theta)\right] \cdot \cos(\phi)$
	$\lvert \boldsymbol{n}\mathbf{f}_{yz^2}\rangle$	$-\frac{1}{8}\sqrt{\frac{5}{2}} \cdot \left[3\,\sin(3\theta) - \sin(\theta)\right] \cdot \sin(\phi)$
	$\lvert \boldsymbol{n}\mathbf{f}_{z^3}\rangle$	$\frac{\sqrt{15}}{2}\,\cos(\theta)\,\sin^2(\theta)$
$\lvert \boldsymbol{n}\mathbf{f}_{xyz;\mathbf{R}}(\theta,\phi)\rangle$	$\lvert \boldsymbol{n}\mathbf{f}_{x(x^2-3y^2)}\rangle$	$-\sqrt{\frac{3}{2}}\,\sin(\theta)\,\cos(\theta)\,\sin(3\phi)$
	$\lvert \boldsymbol{n}\mathbf{f}_{y(3x^2-y^2)}\rangle$	$\sqrt{\frac{3}{2}}\,\sin(\theta)\,\cos(\theta)\,\cos(3\phi)$
	$\lvert \boldsymbol{n}\mathbf{f}_{z(x^2-y^2)}\rangle$	$-2\,\cos(2\theta)\,\sin(\phi)\,\cos(\phi)$
	$\lvert \boldsymbol{n}\mathbf{f}_{xyz}\rangle$	$\cos(2\theta)\,\cos(2\phi)$
	$\lvert \boldsymbol{n}\mathbf{f}_{xz^2}\rangle$	$\sqrt{\frac{5}{2}}\,\sin(\theta)\,\cos(\theta)\,\sin(\phi)$
	$\lvert \boldsymbol{n}\mathbf{f}_{yz^2}\rangle$	$-\sqrt{\frac{5}{2}}\,\sin(\theta)\,\cos(\theta)\,\cos(\phi)$
	$\lvert \boldsymbol{n}\mathbf{f}_{z^3}\rangle$	0

Tab. S4.2: Rotation of atomic $|\mathbf{f}\rangle$ orbitals with arbitrary principal quantum number n by polar and azimuthal angles of θ and ϕ, respectively. The rotations are expressed as angle-dependent linear combinations of atomic orbitals that share the same principal and azimuthal quantum numbers n and $l = 3$. The coefficients have been derived by operation of the rotation matrices $\hat{\mathbf{R}}_y(\theta)$ and $\hat{\mathbf{R}}_z(\phi)$ upon $|\mathbf{f}\rangle$.

	orbitals	**angle-dependent coefficients**
$\|n\mathbf{f}_{xz^2;\mathbf{R}}(\theta,\phi)\rangle$	$\|n\mathbf{f}_{x(x^2-3y^2)}\rangle$	$\frac{\sqrt{15}}{4}\sin^2(\theta)\cos(\theta)\cos(3\phi)$
	$\|n\mathbf{f}_{y(3x^2-y^2)}\rangle$	$\frac{\sqrt{15}}{4}\sin^2(\theta)\cos(\theta)\sin(3\phi)$
	$\|n\mathbf{f}_{z(x^2-y^2)}\rangle$	$\frac{1}{8}\sqrt{\frac{5}{2}}\cdot\left[3\sin(3\theta)-\sin(\theta)\right]\cdot\cos(2\phi)$
	$\|n\mathbf{f}_{xyz}\rangle$	$\frac{1}{4}\sqrt{\frac{5}{2}}\cdot\left[3\sin(3\theta)-\sin(\theta)\right]\cdot\sin(\phi)\cos(\phi)$
	$\|n\mathbf{f}_{xz^2}\rangle$	$\frac{1}{16}\cdot\left[15\cos(3\theta)+\cos(\theta)\right]\cdot\cos(\phi)$
	$\|n\mathbf{f}_{yz^2}\rangle$	$\frac{1}{16}\cdot\left[15\cos(3\theta)+\cos(\theta)\right]\cdot\sin(\phi)$
	$\|n\mathbf{f}_{z^3}\rangle$	$-\frac{1}{8}\sqrt{\frac{3}{2}}\cdot\left[5\sin(3\theta)+\sin(\theta)\right]$
$\|n\mathbf{f}_{yz^2;\mathbf{R}}(\theta,\phi)\rangle$	$\|n\mathbf{f}_{x(x^2-3y^2)}\rangle$	$-\frac{\sqrt{15}}{4}\sin^2(\theta)\sin(3\phi)$
	$\|n\mathbf{f}_{y(3x^2-y^2)}\rangle$	$\frac{\sqrt{15}}{4}\sin^2(\theta)\cos(3\phi)$
	$\|n\mathbf{f}_{z(x^2-y^2)}\rangle$	$-\sqrt{10}\sin(\theta)\cos(\theta)\sin(\phi)\cos(\phi)$
	$\|n\mathbf{f}_{xyz}\rangle$	$\sqrt{\frac{5}{2}}\sin(\theta)\cos(\theta)\cos(2\phi)$
	$\|n\mathbf{f}_{xz^2}\rangle$	$\frac{1}{4}\cdot\left[1-5\cos^2(\theta)\right]\cdot\sin(\phi)$
	$\|n\mathbf{f}_{yz^2}\rangle$	$-\frac{1}{4}\cdot\left[1-5\cos^2(\theta)\right]\cdot\cos(\phi)$
	$\|n\mathbf{f}_{z^3}\rangle$	0
$\|n\mathbf{f}_{z^3;\mathbf{R}}(\theta,\phi)\rangle$	$\|n\mathbf{f}_{x(x^2-3y^2)}\rangle$	$\sqrt{\frac{5}{8}}\sin^3(\theta)\cos(3\phi)$
	$\|n\mathbf{f}_{y(3x^2-y^2)}\rangle$	$\sqrt{\frac{5}{8}}\sin^3(\theta)\sin(3\phi)$
	$\|n\mathbf{f}_{z(x^2-y^2)}\rangle$	$\frac{\sqrt{15}}{2}\sin^2(\theta)\cos(\theta)\cos(2\phi)$
	$\|n\mathbf{f}_{xyz}\rangle$	$\sqrt{15}\sin^2(\theta)\cos(\theta)\sin(\phi)\cos(\phi)$
	$\|n\mathbf{f}_{xz^2}\rangle$	$\frac{1}{2\sqrt{6}}\cdot\left[\sin^3(\theta)+4\sin(3\theta)\right]\cdot\cos(\phi)$
	$\|n\mathbf{f}_{yz^2}\rangle$	$\frac{1}{2\sqrt{6}}\cdot\left[\sin^3(\theta)+4\sin(3\theta)\right]\cdot\sin(\phi)$
	$\|n\mathbf{f}_{z^3}\rangle$	$\frac{1}{2}\cdot\left[\cos^3(\theta)+\cos(3\theta)\right]$

S5 Evaluation of the Scattering Patterns

Here, further details of the evaluation of the scattering patterns in the parabolic eigenstate basis are shown. Since it is assumed that the incident X-ray probe pulse propagates along the y-axis, but the $\boldsymbol{q}$-vector of the $\hat{\boldsymbol{L}}_z$-operator is aligned with the z-axis, it is convenient to interchange the y- and z-coordinates in equation (S17). This change relates the angles θ and ϕ of the rotation directly to the polar and azimuthal angles of the $\boldsymbol{q}$-vector. Hence, the expansions in table S5 are used instead of the expressions for $\left|\boldsymbol{n}\mathbf{d}_{z^2;\mathbf{R}}(\theta,\phi)\right\rangle$ and $\left|\boldsymbol{n}\mathbf{f}_{z^3;\mathbf{R}}(\theta,\phi)\right\rangle$ given in tables S3 and S4.2.

Tab. S5: Rotation of the $\left|\boldsymbol{n}\mathbf{d}_{y^2}\right\rangle$ and $\left|\boldsymbol{n}\mathbf{f}_{y^3}\right\rangle$ vectors with arbitrary principal quantum number n by polar and azimuthal angles of θ and ϕ, respectively. The rotations are expressed as angle-dependent linear combinations of atomic orbitals that share the same principal and azimuthal quantum numbers n and $l = 2$ (**d**) or $l = 3$ (**f**). The coefficients have been derived by operation of the rotation matrices $\hat{\mathbf{R}}_y(\theta)$ and $\hat{\mathbf{R}}_z(\phi)$ upon the two original vectors.

	orbital	**angle-dependent coefficients**
$\left\|\boldsymbol{n}\mathbf{d}_{y^2;\mathbf{R}}(\theta,\phi)\right\rangle$	$\left\|\boldsymbol{n}\mathbf{d}_{x^2-y^2}\right\rangle$	$\frac{\sqrt{3}}{2}\cdot\left[\sin^2(\theta)\,\cos^2(\phi)-\cos^2(\theta)\right]$
	$\left\|\boldsymbol{n}\mathbf{d}_{xy}\right\rangle$	$\frac{\sqrt{3}}{2}\,\sin(2\theta)\,\cos(\phi)$
	$\left\|\boldsymbol{n}\mathbf{d}_{xz}\right\rangle$	$\frac{\sqrt{3}}{2}\,\sin^2(\theta)\,\sin(2\phi)$
	$\left\|\boldsymbol{n}\mathbf{d}_{yz}\right\rangle$	$\frac{\sqrt{3}}{2}\,\sin(2\theta)\,\sin(\phi)$
	$\left\|\boldsymbol{n}\mathbf{d}_{z^2}\right\rangle$	$\frac{1}{2}\cdot\left[3\,\sin^2(\theta)\,\sin^2(\phi)-1\right]$
$\left\|\boldsymbol{n}\mathbf{f}_{y^3;\mathbf{R}}(\theta,\phi)\right\rangle$	$\left\|\boldsymbol{n}\mathbf{f}_{x(x^2-3y^2)}\right\rangle$	$\sqrt{\frac{5}{8}}\,\sin(\theta)\,\cos(\phi)\cdot\left[\sin^2(\theta)\,\cos^2(\phi)-3\,\cos^2(\theta)\right]$
	$\left\|\boldsymbol{n}\mathbf{f}_{y(3x^2-y^2)}\right\rangle$	$\sqrt{\frac{5}{8}}\,\cos(\theta)\cdot\left[3\,\sin^2(\theta)\,\cos^2(\phi)-\cos^2(\theta)\right]$
	$\left\|\boldsymbol{n}\mathbf{f}_{z(x^2-y^2)}\right\rangle$	$\frac{\sqrt{15}}{2}\,\sin(\theta)\,\sin(\phi)\cdot\left[\sin^2(\theta)\,\cos^2(\phi)-\cos^2(\theta)\right]$
	$\left\|\boldsymbol{n}\mathbf{f}_{xyz}\right\rangle$	$\frac{\sqrt{15}}{2}\,\sin^2(\theta)\,\cos(\theta)\,\sin(2\phi)$
	$\left\|\boldsymbol{n}\mathbf{f}_{xz^2}\right\rangle$	$\sqrt{\frac{3}{8}}\,\sin(\theta)\,\cos(\phi)\cdot\left[5\,\sin^2(\theta)\,\sin^2(\phi)-1\right]$
	$\left\|\boldsymbol{n}\mathbf{f}_{yz^2}\right\rangle$	$\sqrt{\frac{3}{8}}\,\cos(\theta)\cdot\left[5\,\sin^2(\theta)\,\sin^2(\phi)-1\right]$
	$\left\|\boldsymbol{n}\mathbf{f}_{z^3}\right\rangle$	$\frac{1}{2}\,\sin(\theta)\,\sin(\phi)\cdot\left[5\,\sin^2(\theta)\,\sin^2(\phi)-3\right]$

Now, the basis vectors in table S5 can be expanded in the parabolic eigenstate basis by application of table S1. After simplification, the two following expressions are obtained:

$$
\begin{aligned}
\left|\mathbf{3d}_{y^2;\mathbf{R}}(\theta,\phi)\right\rangle = &\sqrt{\frac{3}{2}}\cdot\mathrm{Re}\left[\left(\sin(\theta)\,\cos(\phi)-\iota\,\cos(\theta)\right)^2\cdot\left|\mathbf{3,0,0}\right\rangle\right]\\
&+\sqrt{3}\,\sin(\theta)\,\sin(\phi)\cdot\mathrm{Re}\left[\left(\sin(\theta)\,\cos(\phi)-\iota\,\cos(\theta)\right)\cdot\left[\left|\mathbf{3,1,0}\right\rangle-\left|\mathbf{3,0,1}\right\rangle\right]\right]\\
&+\frac{1}{2\sqrt{6}}\cdot\left[3\,\sin^2(\theta)\,\sin^2(\phi)-1\right]\cdot\left[\left|\mathbf{3,2,0}\right\rangle-2\cdot\left|\mathbf{3,1,1}\right\rangle+\left|\mathbf{3,0,2}\right\rangle\right],
\end{aligned}
\tag{S18}
$$

$$
\begin{aligned}
\big|\mathbf{4f}_{y^3;\mathbf{R}}(\theta,\phi)\big\rangle = {} & \frac{\sqrt{5}}{2}\cdot \mathrm{Re}\big[\big(\sin(\theta)\,\cos(\phi) - \iota\,\cos(\theta)\big)^3 \cdot \big|\mathbf{4,0,0}\big\rangle\big] \\
& + \frac{\sqrt{15}}{2}\,\sin(\theta)\,\sin(\phi) \\
& \quad \times \mathrm{Re}\big[\big(\sin(\theta)\,\cos(\phi) - \iota\,\cos(\theta)\big)^2 \cdot \big[\big|\mathbf{4,1,0}\big\rangle - \big|\mathbf{4,0,1}\big\rangle\big]\big] \\
& + \frac{1}{2}\sqrt{\frac{3}{5}}\cdot\big[5\,\sin^2(\theta)\,\sin^2(\phi) - 1\big] \\
& \quad \times \mathrm{Re}\big[\big(\sin(\theta)\,\cos(\phi) - \iota\,\cos(\theta)\big)\cdot\big[\big|\mathbf{4,2,0}\big\rangle - \sqrt{3}\cdot\big|\mathbf{4,1,1}\big\rangle + \big|\mathbf{4,0,2}\big\rangle\big]\big] \\
& + \frac{1}{4\sqrt{5}}\,\sin(\theta)\,\sin(\phi)\cdot\big[5\,\sin^2(\theta)\,\sin^2(\phi) - 3\big] \\
& \quad \times \big[\big|\mathbf{4,3,0}\big\rangle - 3\cdot\big|\mathbf{4,2,1}\big\rangle + 3\cdot\big|\mathbf{4,1,2}\big\rangle - \big|\mathbf{4,0,3}\big\rangle\big].
\end{aligned}
\tag{S19}
$$

Equations (S18) and (S19) can now be inserted into equations (45) to (47) of the paper. After several simplifications, the following expressions for the elements D_3, D_4, and $O_{3,4}$ in the parabolic eigenstate basis are obtained:

$$
\begin{aligned}
D_3 &= \frac{1}{2}\cdot\sum_f^{\infty}\,\big|\big\langle\boldsymbol{\psi}_f\big|\hat{\boldsymbol{L}}_0\big|\mathbf{3d}_{z^2}\big\rangle\big|^2\,W_{f,3,3}(\Delta\omega) \\
&= \frac{1}{2}\cdot\sum_f^{\infty}\,\big|\big\langle\boldsymbol{\psi}_f\big|\hat{\boldsymbol{L}}_z\big|\mathbf{3d}_{y^2;\mathbf{R}}(\theta,\phi)\big\rangle\big|^2\,W_{f,3,3}(\Delta\omega) \\
&= \frac{1}{48}\cdot\big[3\,\sin^2(\theta)\,\sin^2(\phi) - 1\big]^2\cdot\big[\mathcal{D}_{3,0} - 2\,\mathcal{C}_{3,0}\big] \\
&\quad + \frac{3}{4}\cdot\big[\sin^2(\theta)\,\sin^2(\phi) - \sin[\theta]^4\,\sin(\phi)^4\big]\cdot\big[\mathcal{D}_{3,1} - 2\,\mathcal{C}_{3,1}\big] \\
&\quad + \frac{3}{8}\cdot\big[\cos^2(\theta) + \sin^2(\theta)\,\cos^2(\phi)\big]^2\cdot\mathcal{D}_{3,2},
\end{aligned}
\tag{S20}
$$

$$
\begin{aligned}
D_4 &= \frac{1}{2}\cdot\sum_f^{\infty}\,\big|\big\langle\boldsymbol{\psi}_f\big|\hat{\boldsymbol{L}}_0\big|\mathbf{4f}_{z^3}\big\rangle\big|^2\,W_{f,4,4}(\Delta\omega) \\
&= \frac{1}{2}\cdot\sum_f^{\infty}\,\big|\big\langle\boldsymbol{\psi}_f\big|\hat{\boldsymbol{L}}_z\big|\mathbf{4f}_{y^3;\mathbf{R}}(\theta,\phi)\big\rangle\big|^2\,W_{f,4,4}(\Delta\omega) \\
&= \frac{1}{160}\,\sin^2(\theta)\,\sin^2(\phi)\cdot\big[5\,\sin^2(\theta)\,\sin^2(\phi) - 3\big]^2\cdot\big[\mathcal{D}_{4,0} - 2\,\mathcal{C}_{4,0}\big] \\
&\quad + \frac{3}{80}\cdot\big[1 - 5\,\sin^2(\theta)\,\sin^2(\phi)\big]^2\cdot\big[1 - \sin^2(\theta)\,\sin^2(\phi)\big]\cdot\big[\mathcal{D}_{4,1} - 2\,\mathcal{C}_{4,1}\big] \\
&\quad + \frac{15}{16}\,\sin^2(\theta)\,\sin^2(\phi)\cdot\big(1 - \sin^2(\theta)\,\sin^2(\phi)\big)^2\cdot\big[\mathcal{D}_{4,2} - 2\,\mathcal{C}_{4,2}\big] \\
&\quad + \frac{5}{16}\cdot\big[1 - \sin^2(\theta)\,\sin^2(\phi)\big]^3\cdot\mathcal{D}_{4,3},
\end{aligned}
\tag{S21}
$$

$$
\begin{aligned}
O_{3,4} &= \frac{1}{2} \cdot \sum_{f}^{\infty} \left\langle \boldsymbol{\psi}_f \middle| \hat{\boldsymbol{L}}_0 \middle| \mathbf{3d}_{z^2} \right\rangle \left\langle \boldsymbol{\psi}_f \middle| \hat{\boldsymbol{L}}_0 \middle| \mathbf{4f}_{z^3} \right\rangle^* W_{f,3,4}(\Delta\omega) \\
&= \frac{1}{2} \cdot \sum_{f}^{\infty} \left\langle \boldsymbol{\psi}_f \middle| \hat{\boldsymbol{L}}_z \middle| \mathbf{3d}_{y^2;\mathbf{R}}(\theta,\phi) \right\rangle \\
&\qquad \times \left\langle \boldsymbol{\psi}_f \middle| \hat{\boldsymbol{L}}_z \middle| \mathbf{4f}_{y^3;\mathbf{R}}(\theta,\phi) \right\rangle^* W_{f,3,4}(\Delta\omega) \\
&= \frac{1}{16\sqrt{30}} \sin(\theta)\,\sin(\phi) \\
&\quad \times \left[15 \sin^4(\theta)\,\sin^4(\phi) - 14 \sin^2(\theta)\,\sin^2(\phi) + 3\right] \cdot \mathcal{O}_{3,4,0} \\
&\quad + \frac{3}{8\sqrt{5}} \sin(\theta)\,\sin(\phi) \cdot \left[6 \sin^2(\theta)\,\sin^2(\phi)\right. \\
&\qquad\qquad \left. - 5 \sin^4(\theta)\,\sin^4(\phi) - 1\right] \cdot \mathcal{O}_{3,4,1} \\
&\quad + \frac{3}{8}\sqrt{\frac{5}{2}} \sin(\theta)\,\sin(\phi) \cdot \left[\sin^2(\theta)\,\sin^2(\phi) - 1\right]^2 \cdot \mathcal{O}_{3,4,2}.
\end{aligned}
\tag{S22}
$$

The elements in calligraphic letters in equations (S20) to (S22) are defined in tables S6 to S8. The matrix elements they contain can finally be evaluated by means of equations (33) and (34) in the paper.

Tab. S6: Scattering matrix elements $\mathcal{D}_{n,m}$ in the parabolic eigenstate basis. The indices n and m refer to the principal and magnetic quantum numbers. The elements are diagonal in all their quantum numbers. The sums over f involve all parabolic eigenstates with m. The parabolic eigenstates $\boldsymbol{\psi}_{n,n_1,n_2}(\xi,\eta,\varphi)$ are written as $\left|\boldsymbol{n},\boldsymbol{n_1},\boldsymbol{n_2}\right\rangle$. The parabolic quantum numbers n_1 and n_2 obey the relation $n = n_1 + n_2 + m + 1$.

$\mathcal{D}_{3,0} = \sum_f^\infty \Big[\left|\langle \boldsymbol{\psi}_f \vert \hat{\boldsymbol{L}}_z \vert \mathbf{3,2,0} \rangle\right|^2 + 4 \cdot \left|\langle \boldsymbol{\psi}_f \vert \hat{\boldsymbol{L}}_z \vert \mathbf{3,1,1} \rangle\right|^2 + \left|\langle \boldsymbol{\psi}_f \vert \hat{\boldsymbol{L}}_z \vert \mathbf{3,0,2} \rangle\right|^2 \Big] \cdot W_{f,3,3}(\Delta\omega)$
$\mathcal{D}_{3,1} = \sum_f^\infty \Big[\left|\langle \boldsymbol{\psi}_f \vert \hat{\boldsymbol{L}}_z \vert \mathbf{3,1,0} \rangle\right|^2 + \left|\langle \boldsymbol{\psi}_f \vert \hat{\boldsymbol{L}}_z \vert \mathbf{3,0,1} \rangle\right|^2 \Big] \cdot W_{f,3,3}(\Delta\omega)$
$\mathcal{D}_{3,2} = \sum_f^\infty \left|\langle \boldsymbol{\psi}_f \vert \hat{\boldsymbol{L}}_z \vert \mathbf{3,0,0} \rangle\right|^2 \cdot W_{f,3,3}(\Delta\omega)$
$\mathcal{D}_{4,0} = \sum_f^\infty \Big[\left|\langle \boldsymbol{\psi}_f \vert \hat{\boldsymbol{L}}_z \vert \mathbf{4,3,0} \rangle\right|^2 + 9 \cdot \left|\langle \boldsymbol{\psi}_f \vert \hat{\boldsymbol{L}}_z \vert \mathbf{4,2,1} \rangle\right|^2 + 9 \cdot \left|\langle \boldsymbol{\psi}_f \vert \hat{\boldsymbol{L}}_z \vert \mathbf{4,1,2} \rangle\right|^2 + \left|\langle \boldsymbol{\psi}_f \vert \hat{\boldsymbol{L}}_z \vert \mathbf{4,0,3} \rangle\right|^2 \Big] \cdot W_{f,4,4}(\Delta\omega)$
$\mathcal{D}_{4,1} = \sum_f^\infty \Big[\left|\langle \boldsymbol{\psi}_f \vert \hat{\boldsymbol{L}}_z \vert \mathbf{4,2,0} \rangle\right|^2 + 3 \cdot \left|\langle \boldsymbol{\psi}_f \vert \hat{\boldsymbol{L}}_z \vert \mathbf{4,1,1} \rangle\right|^2 + \left|\langle \boldsymbol{\psi}_f \vert \hat{\boldsymbol{L}}_z \vert \mathbf{4,0,2} \rangle\right|^2 \Big] \cdot W_{f,4,4}(\Delta\omega)$
$\mathcal{D}_{4,2} = \sum_f^\infty \Big[\left|\langle \boldsymbol{\psi}_f \vert \hat{\boldsymbol{L}}_z \vert \mathbf{4,1,0} \rangle\right|^2 + \left|\langle \boldsymbol{\psi}_f \vert \hat{\boldsymbol{L}}_z \vert \mathbf{4,0,1} \rangle\right|^2 \Big] \cdot W_{f,4,4}(\Delta\omega)$
$\mathcal{D}_{4,3} = \sum_f^\infty \left|\langle \boldsymbol{\psi}_f \vert \hat{\boldsymbol{L}}_z \vert \mathbf{4,0,0} \rangle\right|^2 \cdot W_{f,4,4}(\Delta\omega)$

Tab. S7: Scattering matrix elements $\mathcal{C}_{n,m}$ in the parabolic eigenstate basis. The indices n and m refer to the principal and magnetic quantum numbers. The elements are off-diagonal in their parabolic quantum numbers, $n_{i,1} \neq n_{j,1}$ and $n_{i,2} \neq n_{j,2}$, but diagonal in n and m. The sums over f involve all parabolic eigenstates with m. The parabolic eigenstates $\boldsymbol{\psi}_{n,n_1,n_2}(\xi,\eta,\varphi)$ are written as $|\boldsymbol{n},\boldsymbol{n_1},\boldsymbol{n_2}\rangle$. The parabolic quantum numbers n_1 and n_2 obey the relation $n = n_1 + n_2 + m + 1$.

$$\begin{aligned}\mathcal{C}_{3,0} = \textstyle\sum_f^\infty \Big[\; & 2\cdot\mathrm{Re}\big[\langle\boldsymbol{\psi}_f|\hat{\boldsymbol{L}}_z|\mathbf{3,1,1}\rangle\,\langle\boldsymbol{\psi}_f|\hat{\boldsymbol{L}}_z|\mathbf{3,2,0}\rangle^*\big]\\ & -\mathrm{Re}\big[\langle\boldsymbol{\psi}_f|\hat{\boldsymbol{L}}_z|\mathbf{3,0,2}\rangle\,\langle\boldsymbol{\psi}_f|\hat{\boldsymbol{L}}_z|\mathbf{3,2,0}\rangle^*\big]\\ & +2\cdot\mathrm{Re}\big[\langle\boldsymbol{\psi}_f|\hat{\boldsymbol{L}}_z|\mathbf{3,0,2}\rangle\,\langle\boldsymbol{\psi}_f|\hat{\boldsymbol{L}}_z|\mathbf{3,1,1}\rangle^*\big]\;\Big]\cdot W_{f,3,3}(\Delta\omega)\end{aligned}$$

$$\mathcal{C}_{3,1} = \textstyle\sum_f^\infty\; \mathrm{Re}\big[\langle\boldsymbol{\psi}_f|\hat{\boldsymbol{L}}_z|\mathbf{3,0,1}\rangle\,\langle\boldsymbol{\psi}_f|\hat{\boldsymbol{L}}_z|\mathbf{3,1,0}\rangle^*\big]\cdot W_{f,3,3}(\Delta\omega)$$

$$\begin{aligned}\mathcal{C}_{4,0} = \textstyle\sum_f^\infty \Big[\; & 3\cdot\mathrm{Re}\big[\langle\boldsymbol{\psi}_f|\hat{\boldsymbol{L}}_z|\mathbf{4,2,1}\rangle\,\langle\boldsymbol{\psi}_f|\hat{\boldsymbol{L}}_z|\mathbf{4,3,0}\rangle^*\big]\\ & -3\cdot\mathrm{Re}\big[\langle\boldsymbol{\psi}_f|\hat{\boldsymbol{L}}_z|\mathbf{4,1,2}\rangle\,\langle\boldsymbol{\psi}_f|\hat{\boldsymbol{L}}_z|\mathbf{4,3,0}\rangle^*\big]\\ & +\mathrm{Re}\big[\langle\boldsymbol{\psi}_f|\hat{\boldsymbol{L}}_z|\mathbf{4,0,3}\rangle\,\langle\boldsymbol{\psi}_f|\hat{\boldsymbol{L}}_z|\mathbf{4,3,0}\rangle^*\big]\\ & +9\cdot\mathrm{Re}\big[\langle\boldsymbol{\psi}_f|\hat{\boldsymbol{L}}_z|\mathbf{4,1,2}\rangle\,\langle\boldsymbol{\psi}_f|\hat{\boldsymbol{L}}_z|\mathbf{4,2,1}\rangle^*\big]\\ & -3\cdot\mathrm{Re}\big[\langle\boldsymbol{\psi}_f|\hat{\boldsymbol{L}}_z|\mathbf{4,0,3}\rangle\,\langle\boldsymbol{\psi}_f|\hat{\boldsymbol{L}}_z|\mathbf{4,2,1}\rangle^*\big]\\ & +3\cdot\mathrm{Re}\big[\langle\boldsymbol{\psi}_f|\hat{\boldsymbol{L}}_z|\mathbf{4,0,3}\rangle\,\langle\boldsymbol{\psi}_f|\hat{\boldsymbol{L}}_z|\mathbf{4,1,2}\rangle^*\big]\;\Big]\cdot W_{f,4,4}(\Delta\omega)\end{aligned}$$

$$\begin{aligned}\mathcal{C}_{4,1} = \textstyle\sum_f^\infty \Big[\; & \sqrt{3}\cdot\mathrm{Re}\big[\langle\boldsymbol{\psi}_f|\hat{\boldsymbol{L}}_z|\mathbf{4,1,1}\rangle\,\langle\boldsymbol{\psi}_f|\hat{\boldsymbol{L}}_z|\mathbf{4,2,0}\rangle^*\big]\\ & -\mathrm{Re}\big[\langle\boldsymbol{\psi}_f|\hat{\boldsymbol{L}}_z|\mathbf{4,0,2}\rangle\,\langle\boldsymbol{\psi}_f|\hat{\boldsymbol{L}}_z|\mathbf{4,2,0}\rangle^*\big]\\ & +\sqrt{3}\cdot\mathrm{Re}\big[\langle\boldsymbol{\psi}_f|\hat{\boldsymbol{L}}_z|\mathbf{4,1,2}\rangle\,\langle\boldsymbol{\psi}_f|\hat{\boldsymbol{L}}_z|\mathbf{4,1,1}\rangle^*\big]\;\Big]\cdot W_{f,4,4}(\Delta\omega)\end{aligned}$$

$$\mathcal{C}_{4,2} = \textstyle\sum_f^\infty\; \mathrm{Re}\big[\langle\boldsymbol{\psi}_f|\hat{\boldsymbol{L}}_z|\mathbf{4,0,1}\rangle\,\langle\boldsymbol{\psi}_f|\hat{\boldsymbol{L}}_z|\mathbf{4,1,0}\rangle^*\big]\cdot W_{f,4,4}(\Delta\omega)$$

Tab. S8: Scattering matrix elements $\mathcal{O}_{n_i,n_j,m}$ in the parabolic eigenstate basis. The indices n_i and n_j refer to the principal quantum numbers of the eigenstates occupied in the wave packet and m is the magnetic quantum number. The elements are off-diagonal in n_i and n_j, $n_i \neq n_j$, but diagonal in m. The sums over f involve all parabolic eigenstates with m. The parabolic eigenstates $\boldsymbol{\psi}_{n,n_1,n_2}(\xi,\eta,\varphi)$ are written as $\left|\boldsymbol{n},\boldsymbol{n_1},\boldsymbol{n_2}\right\rangle$. The parabolic quantum numbers n_1 and n_2 obey the relation $n = n_1 + n_2 + m + 1$.

$$\begin{aligned}
\mathcal{O}_{3,4,0} = \textstyle\sum_f^\infty \Big[& \langle \boldsymbol{\psi}_f|\hat{\boldsymbol{L}}_z|\mathbf{3,2,0}\rangle \langle \boldsymbol{\psi}_f|\hat{\boldsymbol{L}}_z|\mathbf{4,3,0}\rangle^* \\
& - 2\cdot\langle \boldsymbol{\psi}_f|\hat{\boldsymbol{L}}_z|\mathbf{3,1,1}\rangle \langle \boldsymbol{\psi}_f|\hat{\boldsymbol{L}}_z|\mathbf{4,3,0}\rangle^* \\
& + \langle \boldsymbol{\psi}_f|\hat{\boldsymbol{L}}_z|\mathbf{3,0,2}\rangle \langle \boldsymbol{\psi}_f|\hat{\boldsymbol{L}}_z|\mathbf{4,3,0}\rangle^* \\
& - 3\cdot\langle \boldsymbol{\psi}_f|\hat{\boldsymbol{L}}_z|\mathbf{3,2,0}\rangle \langle \boldsymbol{\psi}_f|\hat{\boldsymbol{L}}_z|\mathbf{4,2,1}\rangle^* \\
& + 6\cdot\langle \boldsymbol{\psi}_f|\hat{\boldsymbol{L}}_z|\mathbf{3,1,1}\rangle \langle \boldsymbol{\psi}_f|\hat{\boldsymbol{L}}_z|\mathbf{4,2,1}\rangle^* \\
& - 3\cdot\langle \boldsymbol{\psi}_f|\hat{\boldsymbol{L}}_z|\mathbf{3,0,2}\rangle \langle \boldsymbol{\psi}_f|\hat{\boldsymbol{L}}_z|\mathbf{4,2,1}\rangle^* \\
& + 3\cdot\langle \boldsymbol{\psi}_f|\hat{\boldsymbol{L}}_z|\mathbf{3,2,0}\rangle \langle \boldsymbol{\psi}_f|\hat{\boldsymbol{L}}_z|\mathbf{4,1,2}\rangle^* \\
& - 6\cdot\langle \boldsymbol{\psi}_f|\hat{\boldsymbol{L}}_z|\mathbf{3,1,1}\rangle \langle \boldsymbol{\psi}_f|\hat{\boldsymbol{L}}_z|\mathbf{4,1,2}\rangle^* \\
& + 3\cdot\langle \boldsymbol{\psi}_f|\hat{\boldsymbol{L}}_z|\mathbf{3,0,2}\rangle \langle \boldsymbol{\psi}_f|\hat{\boldsymbol{L}}_z|\mathbf{4,1,2}\rangle^* \\
& - \langle \boldsymbol{\psi}_f|\hat{\boldsymbol{L}}_z|\mathbf{3,2,0}\rangle \langle \boldsymbol{\psi}_f|\hat{\boldsymbol{L}}_z|\mathbf{4,0,3}\rangle^* \\
& + 2\cdot\langle \boldsymbol{\psi}_f|\hat{\boldsymbol{L}}_z|\mathbf{3,1,1}\rangle \langle \boldsymbol{\psi}_f|\hat{\boldsymbol{L}}_z|\mathbf{4,0,3}\rangle^* \\
& - \langle \boldsymbol{\psi}_f|\hat{\boldsymbol{L}}_z|\mathbf{3,0,2}\rangle \langle \boldsymbol{\psi}_f|\hat{\boldsymbol{L}}_z|\mathbf{4,0,3}\rangle^* \Big] \cdot W_{f,3,4}(\Delta\omega)
\end{aligned}$$

$$\begin{aligned}
\mathcal{O}_{3,4,1} = \textstyle\sum_f^\infty \Big[& \langle \boldsymbol{\psi}_f|\hat{\boldsymbol{L}}_z|\mathbf{3,1,0}\rangle \langle \boldsymbol{\psi}_f|\hat{\boldsymbol{L}}_z|\mathbf{4,2,0}\rangle^* \\
& - \langle \boldsymbol{\psi}_f|\hat{\boldsymbol{L}}_z|\mathbf{3,0,1}\rangle \langle \boldsymbol{\psi}_f|\hat{\boldsymbol{L}}_z|\mathbf{4,2,0}\rangle^* \\
& - \sqrt{3}\cdot\langle \boldsymbol{\psi}_f|\hat{\boldsymbol{L}}_z|\mathbf{3,1,0}\rangle \langle \boldsymbol{\psi}_f|\hat{\boldsymbol{L}}_z|\mathbf{4,1,1}\rangle^* \\
& + \sqrt{3}\cdot\langle \boldsymbol{\psi}_f|\hat{\boldsymbol{L}}_z|\mathbf{3,0,1}\rangle \langle \boldsymbol{\psi}_f|\hat{\boldsymbol{L}}_z|\mathbf{4,1,1}\rangle^* \\
& + \langle \boldsymbol{\psi}_f|\hat{\boldsymbol{L}}_z|\mathbf{3,1,0}\rangle \langle \boldsymbol{\psi}_f|\hat{\boldsymbol{L}}_z|\mathbf{4,0,2}\rangle^* \\
& - \langle \boldsymbol{\psi}_f|\hat{\boldsymbol{L}}_z|\mathbf{3,0,1}\rangle \langle \boldsymbol{\psi}_f|\hat{\boldsymbol{L}}_z|\mathbf{4,0,2}\rangle^* \Big] \cdot W_{f,3,4}(\Delta\omega)
\end{aligned}$$

$$\begin{aligned}
\mathcal{O}_{3,4,2} = \textstyle\sum_f^\infty \Big[& \langle \boldsymbol{\psi}_f|\hat{\boldsymbol{L}}_z|\mathbf{3,0,0}\rangle \langle \boldsymbol{\psi}_f|\hat{\boldsymbol{L}}_z|\mathbf{4,1,0}\rangle^* \\
& - \langle \boldsymbol{\psi}_f|\hat{\boldsymbol{L}}_z|\mathbf{3,0,0}\rangle \langle \boldsymbol{\psi}_f|\hat{\boldsymbol{L}}_z|\mathbf{4,0,1}\rangle^* \Big] \cdot W_{f,3,4}(\Delta\omega)
\end{aligned}$$

The matrix structure of the terms in equation (39) is illustrated in figure S1. First, the square on the left represents the equation in the atomic orbital basis with the operator $\hat{\boldsymbol{L}}$. Each of the small, colored squares corresponds to one of the elements in equations (40) to (42). Since the double sum over i and j in equation (6) is restricted to $j > i$, the upper right element is left blank. Secondly, the big square on the right represents the equation in the parabolic eigenstate basis with the operator $\hat{\boldsymbol{L}}_z$. The small squares are filled with the same colors as their related elements on the left. Again, all elements above the main diagonal with $j < i$ do not have to be evaluated and are left blank. Additionally, the matrix is partitioned into several blocks of elements that share the same principal and magnetic quantum numbers. Due to equation (23), all elements in blocks off-diagonal in m are zero and left blank. Hence, out of 256 elements of the full matrix, only 50 have to be considered explicitly. These elements are the terms in tables S6 to S8.

In order to obtain the total number of matrix elements that have to be evaluated, the number of diagonal elements on the left of figure S1 has to be multiplied by the sum of n_f^2 over the principal quantum numbers n_f. In lieu thereof, matrix elements of the operator $\hat{\boldsymbol{L}}_z$ have to fulfill the selection rule $\delta_{m_i m_f}$. The operator only connects to states $\left|\boldsymbol{\psi}_f\right\rangle$ with the same magnetic quantum numbers as the basis states involved in a particular element. Consequently, the numbers of elements diagonal in n and m on the right of figure S1 have to be multiplied by the sum of $n_f - m$ over n_f. As shown in figure S2, the number of matrix elements increases significantly slower with an increasing number of states than in the case of a direct evaluation in the atomic orbital basis with the operator $\hat{\boldsymbol{L}}$.

Here, the sum over f has been truncated at $n_f = 50$. A direct evaluation in the atomic orbital basis would entail 85 850 three-dimensional matrix elements. After expansion of the scattering operator $\hat{\boldsymbol{L}}$ and analytic evaluation of the angular integrals, each matrix element involves $l_f + l_i - \max\left[|l_f - l_i|, |m_f - m_i|\right] + 1$ radial integrals. It appears that a numerical evaluation of 492 550 integrals would be required. The usage of the operator $\hat{\boldsymbol{L}}_z$ and the expansion in the parabolic eigenstate basis permits a reduction of the number of matrix elements by almost 80% to 19 706. Solutions to the latter are provided by equations (28) and (29) and no numerical integration has to be performed. Hence, the computational costs are reduced significantly.

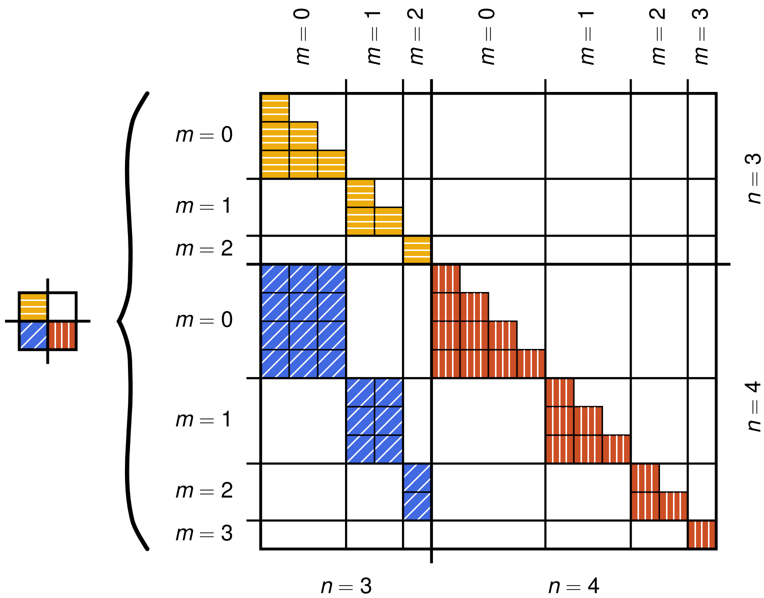

Fig. S1: Matrix structure of the contributions to the differential scattering signal in equation (39). *Left*: atomic orbital basis with $\hat{\boldsymbol{L}}$. *Right*: parabolic eigenstate basis with $\hat{\boldsymbol{L}}_z$. The colored squares represent sums of matrix elements that have to be evaluated and correspond to D_3 (▤), D_4 (▥), and $O_{3,4}$ (▨). The blank parts of the matrices are either redundant or vanish. The matrix in the parabolic eigenstate basis is partitioned into blocks of elements that share the same principal and magnetic quantum numbers m and n, respectively.

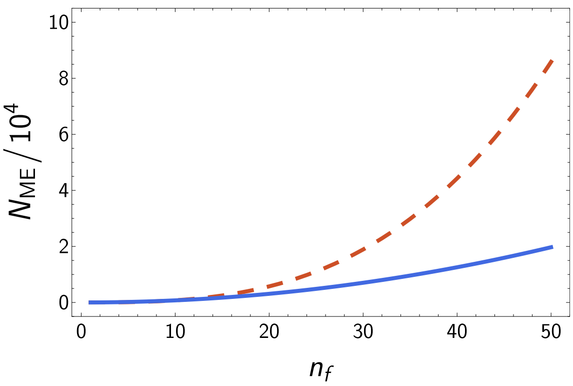

Fig. S2: Number of matrix elements N_{ME} involved in evaluations of equation (39) with increasing number of states $|\psi_f\rangle$. The variable n_f denotes the principal quantum number, at which the sum over f is truncated. Shown are data for an evaluation in the **atomic orbital basis with $\hat{\boldsymbol{L}}$** (---) and an evaluation in the **parabolic eigenstate basis with $\hat{\boldsymbol{L}}_z$** (—). The matrix elements of the former are three-, those of the latter one-dimensional.

S6 Influence of the Pulse Duration

The effect of the pulse duration upon the elastic and inelastic contributions to the static average is shown in figure S3. The inelastic contribution has an optimum, whereas the elastic contribution has not.

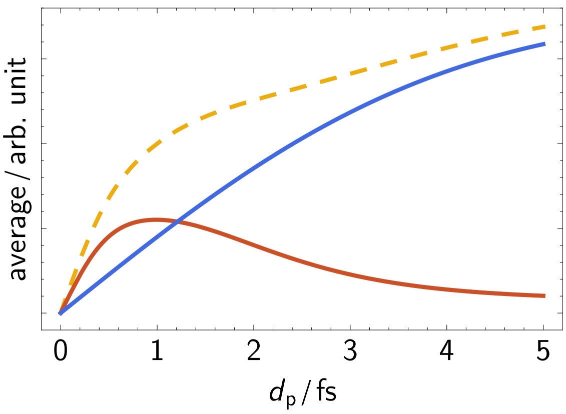

Fig. S3: Elastic (—) and inelastic (—) contributions to the static average (---) of the scattering signal at different probe pulse durations d_p. The signal has been evaluated at $q \approx 0.45/\text{Å}$, $\theta_q \approx 84°$, and $\phi_q = 90°$ with a range of detection of $\pm\Delta\omega = 0.25$ eV around $\langle E_0 \rangle = 4$ keV.